Peer-reviewed version available at Metals 2018, 8, 485; doi:10.3390/met8070485

Article

Microstructural Characterization and Mechanical Properties of 5 vol.% (TiB_w+TiC_p)/Ti Composite Produced by Forging

J.C. Han[1], Z.D. Lü [2], C.J. Zhang[2,*], S.Z. Zhang[2], H.Z. Zhang[3], P. Lin[2], P. Cao[3,**]

[1] School of Mechanical Engineering, Taiyuan University of Technology, Taiyuan 030024, China. hanjianchao@tyut.edu.cn

[2] School of Materials Science and Engineering, Taiyuan University of Technology, Taiyuan 030024, China. zdlv_tyut@163.com; zcj0408@163.com; zhshzh1984@163.com；linpeng@tyut.edu.cn

[3] Department of Chemical and Materials Engineering, University of Auckland, Private Bag 92019, Auckland 1142, New Zealand. hongzhou1229@gmail.com; p.cao@auckland.ac.nz

* Correspondence: zhangchangjiang@tyut.edu.cn Tel.: +86-351-6010022
p.cao@auckland.ac.nz Tel.: +64-9-923-6924

Abstract: In this study, a 5vol. % (TiB_w+TiC_p)/Ti composite pancake with a diameter of 260mm was prepared by casting followed by open die forging in (α+β) phase region. The microstructures of the composite pancake are inhomogeneous, in terms of both matrix microstructure and distribution of reinforcements. The matrix microstructures were gradually refined from the periphery to centre of the pancake. The TiB_w and TiC_p reinforcements tend to be uniformly distributed in the centre region and. It is suggested that the microstructure difference can be mainly ascribed to the temperature variation from the periphery to the centre. Additionally, tensile testing results showed that the centre region of the composite pancake exhibits higher strength than the peripheral region. The strengthening mechanism and the softening behavior of the composite pancake with temperature is discussed.

Keywords: Titanium matrix composites; Microstructure; Mechanical properties; Forging.

1. Introduction

Due to the high elastic modulus, specific strength, superior creep and fatigue resistances, titanium matrix composites (TMCs) have been emerged as attractive candidate materials for high-temperature structural applications in aerospace and automotive industries [1-4]. As one approach to produce TMCs, in situ synthesis techniques have drawn extensive interest because of their superior and isotropic properties along with the ease of fabrication [5-7]. Specifically, among the various reinforcements used in TMCs, TiB whiskers (TiB_w) and TiC particles (TiC_p) are believed to be the most suitable reinforcements since they offer clean interfaces and show thermodynamically stability [8-10]. Currently, combustion assisted cast has been generally adopted to produce in situ TMCs due to the obvious technical advantages [11-13].

However, along with the limited improvement in strength, the in situ TiB_w/Ti or TiC_p/Ti composites prepared by in situ casting routes demonstrate very low room-temperature ductility and poor temperature resistance, which is inadmissible for structural materials [14-15]. Hot working of the TMCs can result in enhanced properties by microstructure refinement and improvement of the distribution of reinforcements [16-17]. However, (TiB_w+TiC_p)/Ti composites are more difficult to process compared with the titanium alloys with minor boron or carbon addition. According to previous studies by Bhat [18] and Liu [19], the non-uniform deformation microstructure and the crack of reinforcements can inevitably come into being for several process variables. The non-uniform miscrostructure and reinforcement cracking will induce deformation incompatibility and flow localization during subsequent forming process and deteriorate the mechanical properties

of final products. Therefore, how to ensure homogeneous deformation microstructure and reduce the microvoids is of significantly importance and needs to be considered during processing of (TiB_w+TiC_p)/Ti composites. In fact, researches on the non-uniform deformation microstructures of Ti alloy [20] and TiAl [21] have been conducted. However, there are no systematic studies available on the microstructural homogeneity and the relative tensile properties of TiB_w/Ti or TiC_p/Ti composites during thermomechanical processing.

In this paper, the as cast 5vol. % (TiB_w+TiC_p)/Ti composite was subjected to (α+β) forging to study microstructural characteristics and relevant tensile properties of the composite pancake within different sampling points.

2. Materials and Methods

The materials used in the experiment was a near-α high-temperature titanium alloy (Ti-6Al-2.5Sn-4Zr-0.7Mo-0.3Si) reinforced with 5 vol.% (TiB_w+TiC_p) reinforcements. The composite ingot was first prepared by induction skull melting (ISM), via the reaction between Ti sponge and B_4C, C powders [5]. The β transus temperature of the composite verified by differential scanning calorimetry (DSC) is approximately 1105°C. A cylindrical billet (Φ130mm×150mm) was cut from the composite ingot by electric discharge machining (EDM). Then the billet was subjected to open die forging, using a hydraulic press at 1050°C with a strain rate of $0.01s^{-1}$ followed by air cooling (the forging process is shown in Fig.1a). Prior to forging, the billet was preheated for 0.5-1h in a resistance furnace and then forged with a total deformation of 75%. Finally, a forged pancake with a diameter of 260 mm and a thickness of 37 mm was obtained without macroscopic cracks (Fig.1b). The composite pancake was cut by EDM for microstructural observation and tensile test. The four sampling points of the as forged composite pancake from periphery to centre are shown in Fig.1c.

The microstructures were characterized by an FEI-Quanta-200F scanning electron microscope (SEM) equipped with electron back scattered diffraction (EBSD) and a Philips-CM12 transmission electron microscope (TEM). The image analysis software Image-Pro Plus was used to investigate the characteristics of the reinforcements and the matrix microstructure. All examinations were performed on the cross-section parallel to the forging direction. For tensile testing, flat tensile specimens were cut from the peripheral region and the central region of the composite pancake. The gauge sections of the room temperature (RT) and elevated temperature tensile specimens were 20mm×6mm×2mm and 20mm×5mm×2mm, respectively. Tensile tests were carried out on an INSTRON-5500R testing machine at 25°C, 600°C, 650°C and 700°C with a constant displacement rate of 8.3×10^{-3}mm s^{-1}. Both at RT and elevated temperature, at least three tensile samples were tested. The tensile properties were reported as an average of the measurements. The fracture surfaces were observed by SEM after tensile tests to investigate the fracture mechanism.

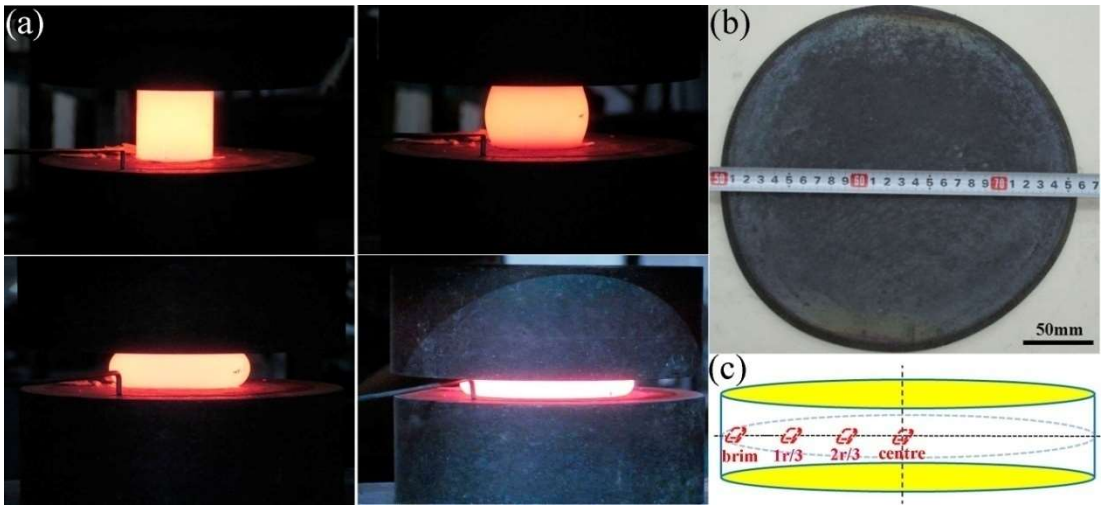

Fig.1 Preparation of the as forged composite pancake: (a) forging process, (b) macrograph of composite pancake, (c) schematic diagram showing the sampling points taken from the composite pancake.

3. Results and discussion

Fig.2 shows the deformation microstructure at different sampling points within the as-forged (TiBw+TiCp)/Ti composite. For the reinforcements, the dominating feature in the peripheral region is the crack of TiBw and TiCp with nearly random distribution. Moreover, the microvoids are usually observed near the ends of the reinforcements, as shown in Fig.2a. At other points from the one third r to the centre, the TiBw and TiCp are more or less aligned perpendicular to the forging direction. In addition, it is worth mentioning that the cracking of the reinforcements mainly occurs at the TiBw whiskers with high aspect ratio rather than at nearly equiaxed TiCp particles. The spaces between the fractured TiBw are filled with matrix leaving no noticeable voids, as shown in Fig.2b-d. Different matrix microstructures were observed at different sampling points. As shown in Fig.2a, the microstructure of the peripheral region is composed of nearly equiaxed α phase and transformed β phase, which does not have any deformation characteristics. Differently from Fig.2a, some coarse and elongated primary α phase appears in Fig.2b, which means that the dynamic recrystallization (DRX) did not proceed completely at the sampling points of one third r. From Fig.2c-d, it can be clearly seen that the microstructures at the sampling points of two thirds r and the centre area are characterized by dominant fine DRX grains plus few transformed β phase.

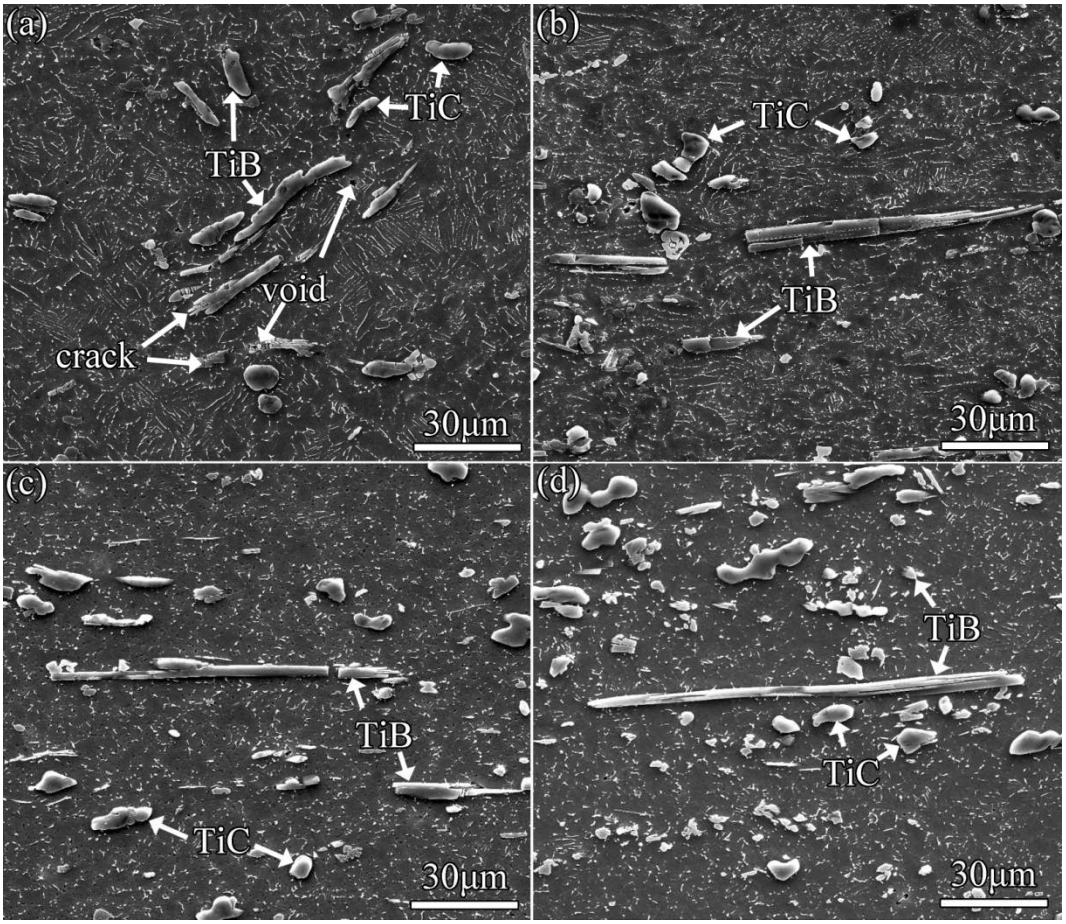

Fig.2 Microstructure homogeneity analysis of the as-forged composite pancake: (a) near brim, (b) at 1/3 radius, (c) at 2/3 radius, (d) near centre.

Preprints (www.preprints.org) | NOT PEER-REVIEWED | Posted: 6 June 2018 doi:10.20944/preprints201806.0074.v1

Peer-reviewed version available at Metals 2018, 8, 485; doi:10.3390/met8070485

The TEM images in Fig. 3 reveals the matrix microstructures of the (TiB_w+TiC_p)/Ti composite pancake. In the peripheral region, the predominant feature in the matrix microstructure is the fine α subgrains. Each α subgrain is surrounded by adjacent α subgrain, as shown in Fig.3a. In addition, it can be seen from Fig.3b that some α subgrains display a large number of dislocations. Theα subgrains are generally induced by dislocation recovery due to the high stored energy generated during forging. However, the matrix microstructures within the centre area are significantly different from those within the periphery. As shown in Fig.3c-d, some fine equiaxed DRX α grains can be clearly seen and the dislocations density appears to be much lower.

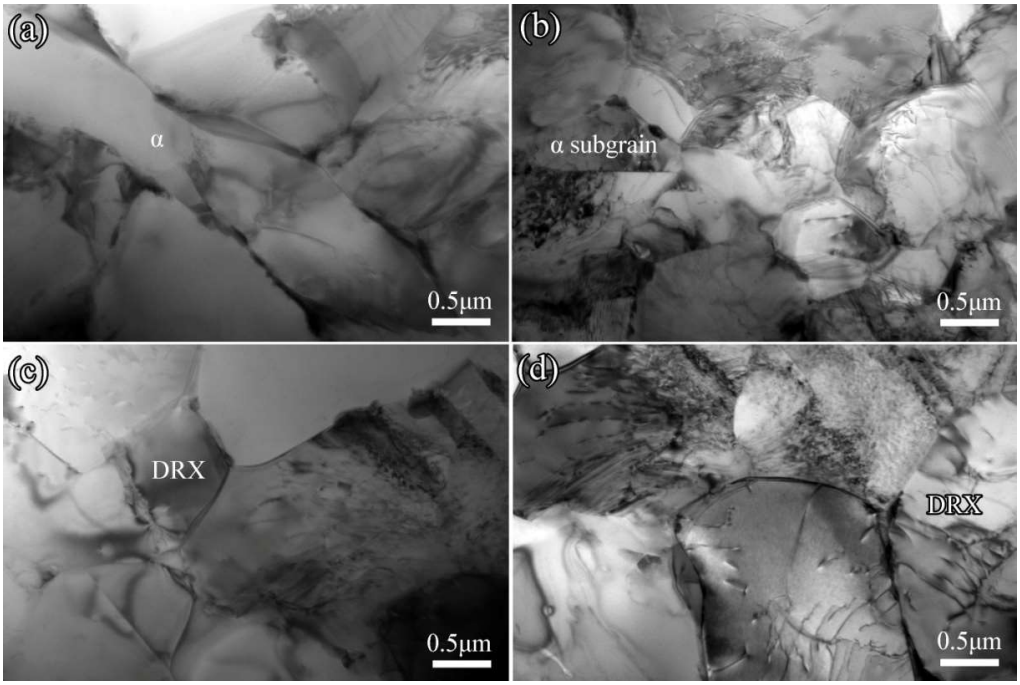

Fig.3 TEM micrographs presenting the matrix microstructure of the (TiB_w+TiC_p)/Ti composite pancake in different sampling points: (a)-(b) near brim, (c)-(d) near centre.

According to Fig.2 and Fig.3, the dynamic recrystallization mainly occurs in the centre region of the composite pancake during forging. Therefore, EBSD images shown in Fig.4 are applied to characterize the matrix microstructure in the centre area. Fig.4a is the inverse pole figure (IPF) map, in which different color codes indicate the different crystal orientation. No obvious texture characteristic exists in the centre area of the composite pancake. Fig.4b presents the grain boundary map overlaid with low ($2°\leq\theta\leq15°$) and high ($\theta\geq15°$) angle boundaries. The low-angle grain boundaries ($2°\leq\theta\leq15°$) described by red and green lines amount for 35.7%, while the high-angle grain boundaries ($\theta\geq15°$) depicted by blue lines occupy 64.3%. Thus, the matrix microstructure is characterized by predominant fine equiaxial DRX grains with some refined subgrains. It is well documented that, high angle boundaries are generally caused by dynamic recrystallization and grain growth, while low angle boundaries are normally the features of substructures generated in the recovery stage. The distribution of the DRX grain size is shown in Fig.4c. Overall, the DRX grain size is no larger than 7μm, and for more than 80 percent of the DRX grains, the grain size is below 4μm. Few DRX grains grow to 7μm, while 23.2% of grains or subgrains are smaller than 2μm. Thus, the coarse casting matrix microstructure of the composite has been effectively broken down by dynamic recrystallization during forging.

Preprints (www.preprints.org) | NOT PEER-REVIEWED | Posted: 6 June 2018 doi:10.20944/preprints201806.0074.v1

Peer-reviewed version available at Metals 2018, 8, 485; doi:10.3390/met8070485

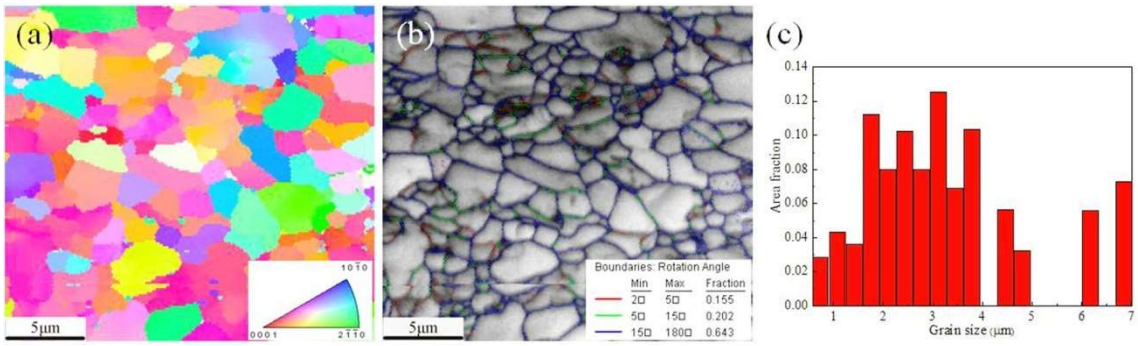

Fig.4 EBSD analyses of the matrix microstructure within the composite pancake: (a) IPF map, (b) grain boundary map and (c) grain size distribution.

3.2 Tensile properties

The tensile properties of the as-forged (TiB_w+TiC_p)/Ti composite samples taken from different sampling points and tested at various temperatures are listed in Table 1. Generally, (α+β) forging effectively improves both the strengths and the elongations, as compared with the as cast (TiB_w+TiC_p)/Ti composite [5]. The tensile properties of the (TiB_w+TiC_p)/Ti composite samples as a function of testing temperature are shown in Fig. 5. In general, the central area of the composite samples exhibits better tensile properties than those within the peripheral area. For example, at room temperature (RT), the ultimate tensile strength (UTS) and elongation to failure (δ) of the sample taken from peripheral region are 1023.7MPa and 1.82%, respectively. For high-temperature testing, the difference in the observed properties is only marginal between the samples taken from different locations. For instance, the UTS of the centre area is just 11MPa higher than that of the peripheral region if tested at 650°C. In addition, it is evident from Fig. 5 that the UTS and elongation of both the brim area and the centre area follow the similar trend, i.e. the strength decreases while the elongation increases with temperature.

Table 1 Room and elevated temperature tensile properties of 5vol.% (TiB_w+TiC_p)/Ti composite pancake with different sampling points.

Sampling points	25°C		600°C		650°C		700°C	
	σ_b (MPa)	δ (%)	σ_b (MPa)	δ (%)	σ_b (MPa)	δ (%)	σ_b (MPa)	δ (%)
near periphery	1023.7	1.82	657.6	5.86	610.9	10.1	493.9	15.3
near centre	1192.1	3.13	701.9	7.78	621.8	14.3	480.5	18.1

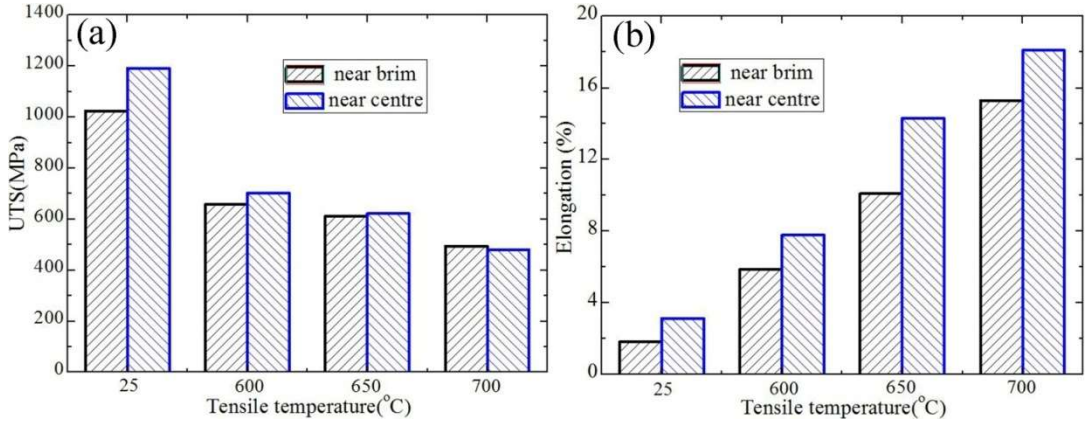

Fig.5. Comparison of tensile properties of the (TiB_w+TiC_p)/Ti composite samples taken from different sampling points , at various tensile temperature: (a) UTS, (b) elongation.

3.3 Fracture morphology

In order to illustrate the fracture characteristics of the 5vol.% (TiB_w+TiC_p)/Ti composite pancake, tensile fracture surfaces of the centre area are taken as an example, which are presented in Fig. 6. As shown in Fig. 6a, the cracked TiB whiskers and TiC particles surrounded by the ductile dimples are observed on the fracture surface. The fracture mode reveals the coexistence of brittle fracture and plastic fracture. It is evident that TiB whiskers and TiC particles embrittle the matrix, with the plastic deformation being very small. In addition, particle pull-out are seldom found on the fracture surface, indicating the good interfacial bonding between the reinforcements and matrix. As the tensile temperature increases to 600◦C and 650◦C, no obvious changes can be noticed except more and deeper dimples in the matrix, as shown in Fig.6b and c. Therefore, there is no significant change in the fracture mechanism of the (TiB_w+TiC_p)/Ti composite when tested at room temperature to 650°C. However, further increasing temperature to 700◦C, there exist distinct features on the fracture surface compared to those found below 700 ◦C. It can be observed in Fig.6 that the dimples dominate the fracture surfaces, indicating the ductile failure at 700◦C. In addition, the pull-outs of TiB whiskers and TiC particles are seen in Fig.6d, revealing a large amount of plastic deformation of matrix exceeds the reinforcements. This result implies that interfacial strength decreases and TiC particles detach from the matrix at the interface at 700◦C.

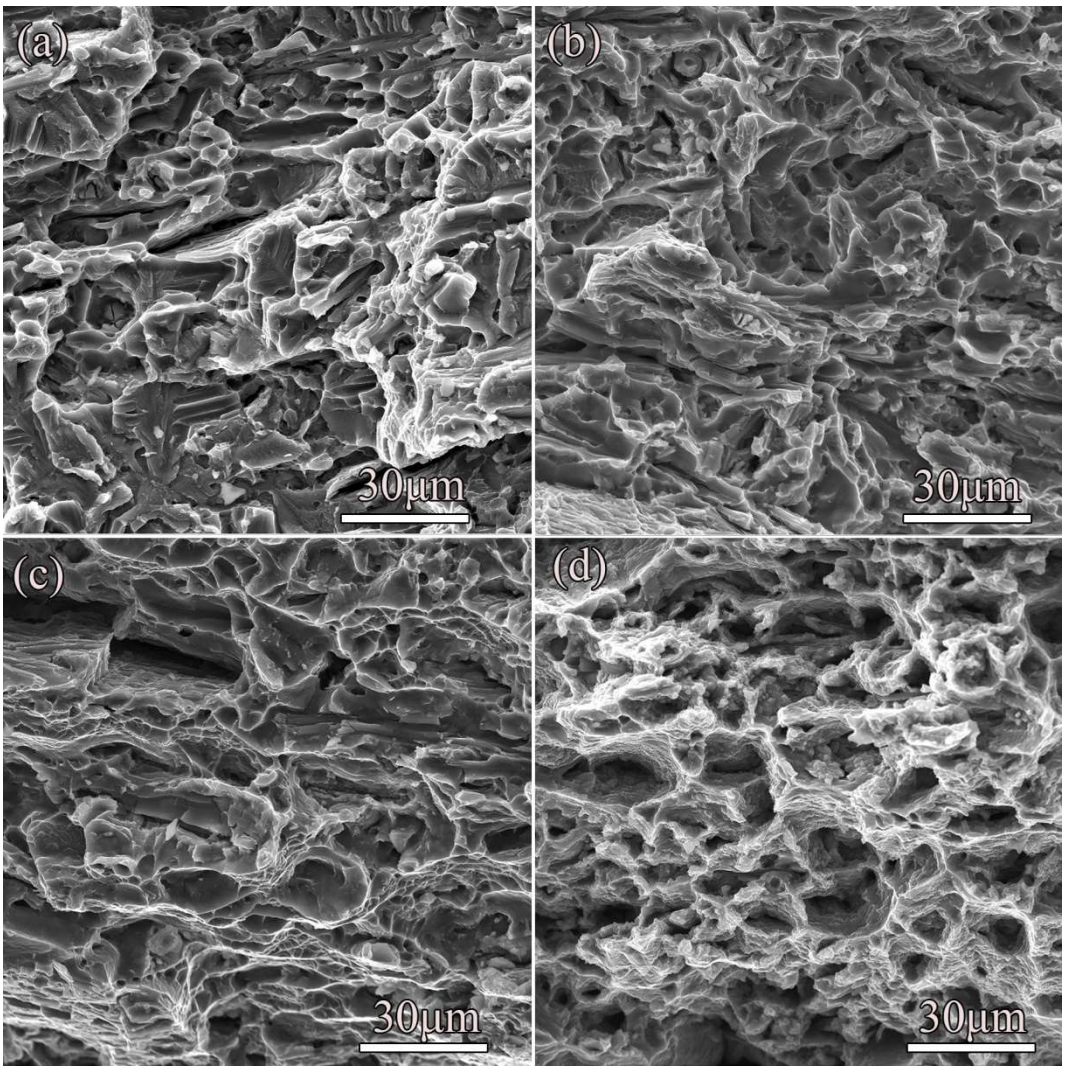

Fig.6 Fracture surfaces of as-forged 5vol.% (TiB_w+TiC_p)/Ti composites at different temperature.(a) room temperature, (b)600 °C, (c)650 °C, (d)700 °C.

4 Discussion

4.1 Microstructure

According to the previous literature [22], the overall section of the forged pancake can be divided into non-deformation region, transition deformation region and homogenous region from the brim area to the centre area. The microstructure difference among these areas can be mainly ascribed to inhomogeneous plastic flow during forging. Generally, various heat transfer processes lead to the temperature drop in the peripheral area [23]. Meanwhile, the temperature at the centre of the billet can be raised due to the large amount of heat produced during plastic deformation and friction. The heat is no easy to dissipate because titanium has a low thermal conductivity [19]. Consequently, the deformation preferentially proceeds in the centre area of the pancake and plastic flow decreases gradually from the center to the brim. Therefore, for the centre area of the (TiB_w+TiC_p)/Ti composite, due to the relatively high deformation degree, the stored energy in the form of dislocation can be high enough to induce dynamic recrystallization of the matrix microstructure, as shown in Fig.2c-d. In contrast, the brim area has smaller amount of the stored energy and relatively low temperature. Thus, the matrix microstructure in the peripheral region does not demonstrate recrystallization features.

As mentioned in Section 3.1, in the brim area of the pancake (Fig.2a), the microvoids located at the ends of the reinforcements are observed while no noticeable voids can be found in the centre area (Fig.2d). In fact, due to the different coefficients of thermal expansion between reinforcements and matrix [24], the stress concentration unavoidably generated during forging can exceed the ultimate strengths of the reinforcements, leading to fracture of the reinforcements. Owing to the positive temperature gradient from brim to centre in the forged pancake, the matrix flow is insufficient to well fill the resulting microvoids at the reinforcements (Fig.2a). While in the centre area, as a result of the relatively high temperature and large deformation, the voids between the reinforcement ends and matrix can be completely closed, as shown in Fig.2d. Similar results were also reported previously [25].

4.2 Tensile properties

In the current study, the strengths of the centre area within the (TiB_w+TiC_p)/Ti composite pancake are superior to those of the brim area. With respect to the strengthening effect, two main factors including grain refinement strengthening and load-carrying capacity of reinforcements, can be considered for the current (TiB_w+TiC_p)/Ti composite [14-15]. According to the classic Hall-Petch theory, the microstructural refinement of matrix can contribute to the improvement in the tensile strength below equi-cohesive temperature [26]. Therefore, strengthening effect caused by grain refinement of the current composite both at room temperature and 600°C can be discussed together because of that the equicohesive temperature of the matrix alloy within the composite can be regarded as 600°C [27]. As depicted in Fig.2, the coarse matrix microstructure of the brim area (Fig.2a) is gradually refined to equiaxed DRX grains accompanied by the reduction in the size of α grains (Fig.2d). Therefore the tensile strength of the composite is increased. Additionally, the enhancement in strengths can be partially owing to load-bearing effect arising from TiB_w and TiC_p reinforcements. The micrographs of fracture surfaces presented in Fig.6a and b reveal that most of the TiB_w and TiC_p fracture during tensile test, indicating the interfacial bonding is strong enough to transfer load from matrix to reinforcements. As shown in Fig.2d, the relatively evenly distributed TiB_w and TiC_p shown in the centre area undoubtedly improve the tensile strengths. Therefore, the centre area of the pancake exhibits higher tensile strengths than those within the brim area at a temperature from room temperature to 600°C.

At a temperature above 600°C, the composite samples still have high strength. This is due to the load-carrying capacity of TiB_w and TiC_p. Boehlert et al. [28] suggested that the load-sharing mechanism requires a good interface bonding between the matrix alloy and the reinforcement. This has been evidenced in Fig.6c. Ma [29] and Zhang [30] believed that the strengthening effect of reinforcements becomes more profound at high temperatures. In other words, the TiB_w and TiC_p tend to fracture prematurely under stress at low temperatures while the stress around the reinforcements can be released by the ductile matrix at higher temperatures. Therefore, the load transferring effect becomes more remarkable at 650°C, leading to the superior tensile strength of the centre area within the pancake. As the tensile temperature increases to 700°C, the prevailing characteristic of interfacial debonding shown in Fig.6d implies that load-carrying of TiB_w and TiC_p ceases. As a result, the centre area exhibits lower strength, as compared with the peripheral region.

5. Conclusions

The following conclusions can be drawn from this study:

1. The as-forged 5vol.% (TiB_w+TiC_p)/Ti pancake exhibits inhomogeneous microstructure, with residual transformed β microstructure and microvoids near the randomly distributed TiB_w and TiC_p existing in the peripheral area.

2. The microstructure in the centre area consists of dominant DRX grains plus some refined subgrains and dislocations. The grain size ranges between 1μm and 7μm. Moreover, the TiB_w and TiC_p are uniformly distributed within the matrix.

3. Overall, the tensile properties of the composite samples taken from the central area of the pancake are better than those of the samples taken from the peripheral area. Grain refinement strengthening and load-carrying capacity of TiB_w and TiC_p independently or collectively dominate the strengthening mechanism.

Acknowledgement: The authors gratefully thank the financial support from the National Natural Science Foundation of China (Nos.51504163 and 51604191).

Author Contributions: All authors have contributed significantly. Changjiang Zhang, Peng Cao and Jianchao Han designed the project. Zhidan Lü, Jianchao Han, Hongzhou Zhang, Shuzhi Zhang undertook the experiments and data collection. Peng Lin, Zhidan Lü and Changjiang Zhang analyzed the data. All authors contributed to the discussion of the results. Jianchao Han, Changjiang Zhang and Peng Cao wrote and revised the manuscript.
Conflicts of Interest: The authors declare no conflict of interest.

References

1. Huang L.Q.; Qian M.; Liu Z.M.; Nguyen V.T.; Yang L.; Wang L.H.; Zou J. In situ preparation of TiB nanowires for high-performance Ti metal matrix nanocomposites. J. Alloy. Compd. ***2018,*** *735,* 2640.
2. Tjong S.C.; Mai Y.M. Processing-structure-property aspects of particulate and whisker-reinforced titanium matrix composites. Compos. Sci. Technol. ***2008,*** *68,* 583**.**
3. Huang L.Q.; Wang L.H.; Qian M.; Zou J. High tensile-strength and ductile titanium matrix composites strengthened by TiB nanowires. Scr. Mater. ***2017,*** *141,* 133.
4. Ozerov M.; Klimova M.; Kolesnikov A.; Stepanov N.; Zherebtsov S. Deformation behavior and microstructure evolution of a Ti/TiB metal-matrix composite during high-temperature compression tests. Mater. Des. ***2016,*** *112,* 17.
5. Zhang C.J.; Kong F.T.; Xiao S.L.; Zhao E.T.; Xu L.J.; Chen Y.Y. Evolution of microstructure and tensile properties of in situ titanium matrix composites with volume fraction of (TiB+TiC) reinforcements. Mater. Sci. Eng. A ***2012,*** *548,* 152.
6. Liu Y.; Ding J.; Qu W.; Su Y.; Yu Z., Microstructure Evolution of TiC particles in situ, synthesized by laser cladding. Materials. ***2017,*** *10,* 281.
7. Huang L.J.; Geng L.; Peng H.X.; In situ (TiB_w+TiC_p)/Ti6Al4V composites with a network reinforcement distribution. Mater. Sci. Eng. A ***2010*** *527* 6723.
8. Zhang W.C.; Wang M.M.; Chen W.Z.; Feng Y.J.; Yu Y. Preparation of TiB_w/Ti-6Al-4V composite with an inhomogeneous reinforced structure by a canned hot extrusion process. J. Alloy. Compd. ***2016,*** *669,* 79.
9. Li S.F.; Kondoh K.; Imai H.; Chen B.; Jia L.; Umeda J. Microstructure and mechanical properties of P/M titanium matrix composites reinforced by in-situ synthesized TiC-TiB. Mater. Sci. Eng. A ***2015,*** *628,* 75.
10. Tabrizi S.G.; Sajjadi S.A.; Babakhani A.; Lu W. Influence of spark plasma sintering and subsequent hot rolling on microstructure and flexural behavior of in-situ TiB and TiC reinforced Ti6Al4V composite. Mater. Sci. Eng. A ***2015,*** *624,* 271.
11. Qi J.Q.; Sui Y.W.; Chang Y.; He Y.Z.; Wei F.X.; Meng Q.K.; Wei Z.J. Microstructural characterization and mechanical properties of TiC/near-α Ti composite obtained at slow cooling rate. Mater. Charact. ***2016,****118,* 263.
12. Qi J.Q.; Chang Y.; He Y.Z.; Sui Y.W.; Wei F.X.; Meng Q.K.; Wei Z.J. Effect of Zr, Mo and TiC on microstructure and high-temperature tensile strength of cast titanium matrix composites. Mater. Des. ***2016,*** *99,* 421.
13. Yang Z.F.; Lu W.J.; Zhao L.; Qin J.N.; Zhang D. Microstructure and mechanical property of in situ synthesized multiple-reinforced (TiB+TiC+La_2O_3)/Ti composites. J. Alloy. Compd. ***2008,*** *455,* 210.
14. Zhang C.J.; Zhang S.Z.; Lin P.; Hou Z.P.; Kong F.T.; Chen Y.Y. Thermomechanical processing of (TiB+TiC)/Ti matrix composites and effects on microstructure and tensile properties. J. Mater. Res. ***2016,*** *31,* 1244.

15. Chandravanshi V.K.; Sarkar R.; Ghosal P.; Kamat S.V.; Nandy T.K. Effect of minor additions of boron on microstructure and mechanical properties of as-cast near α titanium alloy. Metall. Mater. Trans. A ***2010,*** *41,* 936.
16. Morsi K.; Patel V.V. Processing and properties of titanium-titanium boride (TiB_w) matrix composites- a review. J. Mater. Sci. ***2007,*** *42,* 2037.
17. Imayev V.; Gaisin R;. Gaisina E.; Imayev R.; Fecht H. J.; Pyczak F. Effect of hot forging on microstructure and tensile properties of Ti-TiB based composites produced by casting. Mater. Sci. Eng. A ***2014,*** *609,* 34.
18. Bhat R.B.; Tamirisakandala S.; Miracle D.B.; Ravi V.A. Thermomechanical response of a powder metallurgy Ti-6Al-4V alloy modified with 2.9 pct boron. Metall. Mater. Trans. A ***2005,*** *36,* 845.
19. Liu B.; Li Y. P.; Matsumoto H.; Liu Y. B.; Liu Y.; Tang H. P.; Chiba A. Thermomechanical response of particulate-reinforced powder metallurgy titanium matrix composites-A study using processing map. Mater. Sci. Eng. A ***2010,*** *527,* 4733.
20. Huang D.M.; Wang H.L.; Chen X.; Chen Y.; Guo H. Influence of forging process on microstructure and mechanical properties of large section Ti-6.5 Al-1Mo-1V-2Zr alloy bars. T. Nonferr. Metal. Soc. ***2013,*** *23,* 2276.
21. Niu H.Z.; Kong F.T.; Chen Y.Y. Microstructure characterization and tensile properties of β phase containing TiAl pancake. J. Alloy. Compd. ***2011,*** *509,* 10179.
22. Huang L.J.; Zhang Y.Z.; Geng L.; Wang B.; Ren W. Hot compression characteristics of TiB_w/Ti6Al4V composites with novel network microstructure using processing maps. Mater. Sci. Eng. A ***2013,****580,* 242.
23. Zhou W.; Ge P.; Zhao Y.Q. Finite element analysis of temperature field in forging process of Ti-1023 alloy. Hot. Working. Technol. ***2009,*** *38,* 21.
24. Roy S.; Suwas S. The influence of temperature and strain rate on the deformation response and microstructural evolution during hot compression of a titanium alloy Ti-6Al-4V-0.1 B. J. Alloy. Compd. ***2013,*** *548,* 110.
25. Srinivasan R.; Bennett M.D.; Tamirsakandala S. Rolling of plates and sheets from as-cast Ti-6Al-4V-0.1B. J. Mater. Eng. Perform. ***2008,*** *18,* 390.
26. Armstrong R.; Codd I.; Douthwaite R.M.; Petch N.J. The plastic deformation of polycrystalline aggregates. Phil. Mag. ***1962,*** *7,* 45.
27. Xiao L.; Lu W.J.; Qin J.N. High-temperature tensile properties of in situ-synthesized titanium matrix composites with strong dependence on strain rates. J. Mater. Res. ***2008,*** *23,* 3066.
28. Boehlert C.J.; Tamirisakandala S.; Curtin W.A.; Miracle D.B. Assessment of in situ TiB whisker tensile strength and optimization of TiB-reinforced titanium alloy design. Scr. Mater. ***2009,*** *61,* 245.
29. Ma F.C.; Lu W.J.; Qin J.N.; Zhang D. Strengthening mechanisms of carbon element in in situ TiC/Ti-1100 composites. J. Mater. Sci. ***2006,*** *41,* 5395.
30. Zhang C.J.; Kong F.T.; Xu L.J.; Zhao E.T.; Xiao S.L.; Chen Y.Y. Temperature dependence of tensile properties and fracture behavior of as rolled TiB/Ti composite sheet. Mater. Sci. Eng. A ***2012,*** *556,* 962.